J|A|C|S
ARTICLES

Published on Web 12/19/2008

Quantum Chemical Modeling of Zeolite-Catalyzed Methylation Reactions: Toward Chemical Accuracy for Barriers

Stian Svelle,*,† Christian Tuma,‡ Xavier Rozanska,‡ Torsten Kerber,‡ and
Joachim Sauer*,‡

inGAP Center of Research Based Innovation, Department of Chemistry, University of Oslo,
P.O. Box 1033 Blindern, N-0315 Oslo, Norway, and Humboldt-Universität zu Berlin, Institut für
Chemie, Unter den Linden 6, D-10099 Berlin, Germany

Received September 29, 2008; E-mail: stian.svelle@kjemi.uio.no; sek.qc@chemie.hu-berlin.de

Abstract: The methylation of ethene, propene, and *t*-2-butene by methanol over the acidic microporous H-ZSM-5 catalyst has been investigated by a range of computational methods. Density functional theory (DFT) with periodic boundary conditions (PBE functional) fails to describe the experimentally determined decrease of apparent energy barriers with the alkene size due to inadequate description of dispersion forces. Adding a damped dispersion term expressed as a parametrized sum over atom pair C_6 contributions leads to uniformly underestimated barriers due to self-interaction errors. A hybrid MP2:DFT scheme is presented that combines MP2 energy calculations on a series of cluster models of increasing size with periodic DFT calculations, which allows extrapolation to the periodic MP2 limit. Additionally, errors caused by the use of finite basis sets, contributions of higher order correlation effects, zero-point vibrational energy, and thermal contributions to the enthalpy were evaluated and added to the “periodic” MP2 estimate. This multistep approach leads to enthalpy barriers at 623 K of 104, 77, and 48 kJ/mol for ethene, propene, and *t*-2-butene, respectively, which deviate from the experimentally measured values by 0, +13, and +8 kJ/mol. Hence, enthalpy barriers can be calculated with near chemical accuracy, which constitutes significant progress in the quantum chemical modeling of reactions in heterogeneous catalysis in general and microporous zeolites in particular.

1. Introduction

Synthesis and conversion of hydrocarbon molecules by solid acid catalysts in general and by zeolites in particular belong to the industrially most important catalytic processes,[1] but the underlying reaction mechanisms are a persistent scientific challenge. A prominent example is the conversion of methanol to hydrocarbons over H-ZSM-5 zeolite catalysts,[2] which was first discovered and commercialized by Mobil Oil in 1986.[3] Later, Haldor Topsøe developed the Topsøe integrated gasoline synthesis (TIGAS) process,[4] Lurgi the methanol to propene (MTP) process,[5] and Norsk Hydro/UOP the methanol to olefins (MTO) process (based on the SAPO-34 catalyst).[6]

While initial research focused on the first C−C bond formation, that is, on how two (or more) methanol molecules could combine to give initial alkenes and water,[2] Dahl and Kolboe[7,8] proposed the hydrocarbon pool mechanism, which assumes that light alkenes are formed via repeated methylation and dealkylation reactions of aromatic reaction centers.[9,10] Very recent studies have unraveled more details showing that methanol carbon atoms are to a considerable extent incorporated in the C_{3+} alkenes in a parallel alkene methylation/cracking cycle[11,12] related to the scheme originally proposed by Dessau.[13] Hence, alkene methylation reactions (Scheme 1), which are the focus of the present study, are key steps in the conversion of methanol to hydrocarbons (MTH) over the archetype H-ZSM-5 catalyst.

Scheme 1. Methylation of Ethene with Methanol To Yield Propene and Water

Computational studies based on quantum chemical calculations and transition state theory for individual steps (and combined with microkinetic modeling of the whole reaction network in a later stage) can make significant contributions to

---

† University of Oslo.
‡ Humboldt-Universität zu Berlin.

(1) Corma, A. *Chem. Rev.* **1995**, *95*, 559–614.
(2) Stöcker, M. *Microporous Mesoporous Mater.* **1999**, *29*, 3–48.
(3) Cobb, J. In *New Zealand Synfuel: The Story of the World's First Natural Gas to Gasoline Plant*; Connell, G., Ed.; Cobb/Horwood Publications: Auckland, New Zealand, 1995; p 1.
(4) Topp-Jørgensen, J. *Stud. Surf. Sci. Catal.* **1988**, *36*, 293–305.
(5) Koempel, H.; Liebner, W. *Stud. Surf. Sci. Catal.* **2007**, *167*, 261–267.
(6) Chen, J. Q.; Bozzano, A.; Glover, B.; Fuglerud, T.; Kvisle, S. *Catal. Today* **2005**, *106*, 103–107.
(7) Dahl, I. M.; Kolboe, S. *Catal. Lett.* **1993**, *20*, 329–336.
(8) Dahl, I. M.; Kolboe, S. *J. Catal.* **1994**, *149*, 458–464.
(9) Haw, J. F.; Song, W.; Marcus, D. M.; Nicholas, J. B. *Acc. Chem. Res.* **2003**, *36*, 317–326.
(10) Olsbye, U.; Bjørgen, M.; Svelle, S.; Lillerud, K.-P.; Kolboe, S. *Catal. Today* **2005**, *106*, 108–111.
(11) Svelle, S.; Joensen, F.; Nerlov, J.; Olsbye, U.; Lillerud, K.-P.; Kolboe, S.; Bjorgen, M. *J. Am. Chem. Soc.* **2006**, *128*, 14770–14771.
(12) Bjørgen, M.; Svelle, S.; Joensen, F.; Nerlov, J.; Kolboe, S.; Bonino, F.; Palumbo, L.; Bordiga, S.; Olsbye, U. *J. Catal.* **2007**, *249*, 195–207.
(13) Dessau, R. M. *J. Catal.* **1986**, *99*, 111–116.

10.1021/ja807695p CCC: $40.75

the understanding of such complex reactions on surfaces. Density functional theory (DFT) is the current method of choice for studies of chemical systems of extended size and complexity. In particular, implementations with periodic boundary conditions (PBC) using plane wave basis sets and generalized gradient approximation (GGA) type functionals became very popular for the investigation of reactions occurring on surfaces or within a porous solid. However, commonly used density functionals suffer from deficiencies for the description of long-range dispersion interactions[14,15] and self-interaction correction,[16,17] which result in underestimated adsorption energies and systematically too low energy barriers, respectively.[18] A pragmatic solution is available for the first problem: adding a damped dispersion term as parametrized sum over atom pair C_6 contributions to, for example, PBE or BLYP DFT results.[19,20] This approach, denoted DFT-D, has been shown to work well for noncovalently bonded complexes and large molecules,[21] as well as for solid state[22−24] and adsorption problems.[24] The second problem can be diminished by passing to hybrid functionals including Fock exchange such as PBE0 or B3LYP, or by using even more sophisticated parametrized functionals.[18] When plane wave basis sets are employed, the use of hybrid functionals is computationally much more expensive as compared to GGA-type functionals and becomes prohibitive for large systems under periodic boundary conditions. Here, we follow a different approach and pass to wave function-based electron correlation methods. The method of choice would be coupled-cluster calculations including single, double, and perturbatively treated connected triple excitations, CCSD(T), but even the simplest method, second-order Møller−Plesset perturbation theory (MP2), provides a substantial improvement on both problems if nearly degenerate electronic structures are avoided. It usually shows smaller errors on barriers than GGA type functionals (see Table 5 of ref 18) and describes dispersion interactions explicitly. The acid-catalyzed reactions studied here do not involve decoupling of electron pairs, and, as we will show below for small zeolite models, differences between MP2 and CCSD(T) energy barriers are tiny, 2% or less.

For periodic systems, however, even MP2 calculations are presently feasible only with small basis sets for few atoms in the unit cell.[25,26] We therefore rely on a hybrid QM:QM scheme that combines MP2 calculations with Gaussian basis sets for the reaction site and plane wave basis set DFT for the full system under periodic boundary conditions.[27,28] For a series of cluster models (**C**) of increasing size representing the active site of the full periodic system (**S**), both MP2 and DFT calculations are performed. The size-dependent "high-level" correction, defined as the difference between MP2 and DFT energies,

$$\Delta E(\mathbf{C})_{\mathrm{high}} = E(\mathbf{C})_{\mathrm{MP2}} - E(\mathbf{C})_{\mathrm{DFT}} \tag{1}$$

is extrapolated to the periodic model limit, $\Delta E(\mathbf{S})_{\mathrm{high}}$. When added to the DFT energy for the periodic structure, $E(\mathbf{S})_{\mathrm{DFT}}$, an estimate of MP2 quality for the energy of the periodic structure is obtained,

$$E(\mathbf{S})_{\mathrm{MP2}} \approx E(\mathbf{S})_{\mathrm{DFT}} + \Delta E(\mathbf{S})_{\mathrm{high}} \tag{2}$$

In previous applications to proton jump reactions in hydrated and dry zeolite H-SSZ-13[27] or to physisorption and chemisorption of iso-butene in zeolite H-Ferrierite,[28] substantial improvement over DFT (PBE) results was achieved when using the hybrid MP2:DFT scheme.

Here, we apply the hybrid MP2:DFT method to study the methylation of ethene, propene, and *t*-2-butene over zeolite H-ZSM-5 for which reaction rates and activation energies are known from experiment.[29,30] We will show that hybrid MP2:DFT is able to reproduce enthalpy barriers and alkene chain length trends on these barriers in important steps of the MTH reaction mechanism with near chemical accuracy (mean error 6 kJ/mol). Plain DFT (PBE) fails to reproduce the lowering of the barrier from ethene to propene and *t*-2-butene (because of missing long-range dispersion contributions), whereas PBE+dispersion (DFT-D) results are systematically too low (mean error −17 kJ/mol) because of self-interaction correction errors.

The hybrid MP2:DFT method presented here is computationally expensive and not suited for routine studies on many systems, but it will play an important role in generating reliable data on which parametrizations for reactive force[31] fields and hybrid QM:force field methods[32−34] can be based.

The methylation of ethene, propene, the four butene isomers, and 2-methyl-2-butene was investigated previously with DFT adopting a small four-tetrahedra cluster model.[35] In qualitative agreement with experiment,[29,30] the calculated activation barriers were dependent on the size and substitution pattern of the alkene reactant, but the quantitative agreement was poor. In their DFT study on methylation of toluene, Vos et al.[36,37] found that cluster calculations significantly overestimate barriers relative to periodic calculations. They recognized that DFT with standard functionals does not yield accurate adsorption energies, which, in turn, affects apparent barrier heights. DFT studies have also been made for the methylation of aromatics on small cluster models,[38] on cluster models embedded in larger portions of the ZSM-5 structure (44−46 tetrahedra) using the ONIOM

---

(14) Wesolowski, T. A.; Parisel, O.; Ellinger, Y.; Weber, J. *J. Phys. Chem. A* **1997**, *101*, 7818–7825.
(15) Zhang, Y.; Pan, W.; Yang, W. *J. Chem. Phys.* **1997**, *107*, 7921–7925.
(16) Gritsenko, O. V.; Ensing, B.; Schipper, P. R. T.; Baerends, E. J. *J. Phys. Chem. A* **2000**, *104*, 8558–8565.
(17) Porezag, D.; Pederson, M. R. *J. Chem. Phys.* **1995**, *102*, 9345–9349.
(18) Zhao, Y.; Truhlar, D. G. *J. Phys. Chem. A* **2005**, *109*, 5656–5667.
(19) Grimme, S. *J. Comput. Chem.* **2004**, *25*, 1463–1473.
(20) Grimme, S. *J. Comput. Chem.* **2006**, *27*, 17873–1799.
(21) Schwabe, T.; Grimme, S. *Acc. Chem. Res.* **2008**, *41*, 569–579.
(22) Ortmann, F.; Bechstedt, F.; Schmidt, W. G. *Phys. Rev. B* **2006**, *73*, 205101/1–205101/10.
(23) Civalleri, B.; Zicovich-Wilson, C. M.; Valenzano, L.; Ugliengo, P. *Cryst. Eng. Commun.* **2008**, *10*, 405–410.
(24) Kerber, T.; Sierka, M.; Sauer, J. *J. Comput. Chem.* **2008**, *29*, 2088–2097.
(25) Casassa, S.; Halo, M.; Maschio, L.; Roetti, C.; Pisani, C. *Theor. Chem. Acc.* **2007**, *117*, 781–791.
(26) Maschio, L.; Usvyat, D.; Manby, F. R.; Casassa, S.; Pisani, C.; Schütz, M. *Phys. Rev. B* **2007**, *76*, 075101/1–075101/9.
(27) Tuma, C.; Sauer, J. *Chem. Phys. Lett.* **2004**, *387*, 388–394.
(28) Tuma, C.; Sauer, J. *Phys. Chem. Chem. Phys.* **2006**, *8*, 3955–3965.
(29) Svelle, S.; Rønning, P. O.; Kolboe, S. *J. Catal.* **2004**, *224*, 115–123.
(30) Svelle, S.; Rønning, P. O.; Olsbye, U.; Kolboe, S. *J. Catal.* **2005**, *234*, 385–400.
(31) van Duin, A. C. T.; Strachan, A.; Stewman, S.; Zhang, Q. S.; Xu, X.; Goddard, W. A. *J. Phys. Chem. A* **2003**, *107*, 3803–3811.
(32) Clark, L. A.; Sierka, M.; Sauer, J. *J. Am. Chem. Soc.* **2004**, *126*, 936–947.
(33) Clark, L. A.; Sierka, M.; Sauer, J. *J. Am. Chem. Soc.* **2003**, *125*, 2136–2141.
(34) De Moor, B.; Reyniers, M.-F.; Sierka, M.; Sauer, J.; Marin, G. B. *J. Phys. Chem. C* **2008**, *112*, 11796–11812.
(35) Svelle, S.; Arstad, B.; Kolboe, S.; Swang, O. *J. Phys. Chem. B* **2003**, *107*, 9281–9289.
(36) Vos, A. M.; Rozanska, X.; Schoonheydt, R. A.; van Santen, R. A.; Hutschka, F.; Hafner, J. *J. Am. Chem. Soc.* **2001**, *123*, 2799–2809.
(37) Vos, A. M.; Nulens, K. H. L.; De Proft, F.; Schoonheydt, R. A.; Geerlings, P. *J. Phys. Chem. B* **2002**, *106*, 2026–2034.
(38) Arstad, B.; Swang, O.; Kolboe, S. *J. Phys. Chem. B* **2002**, *106*, 12722–12726.

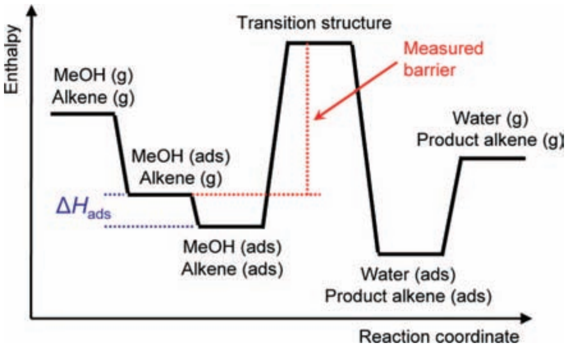

Figure 1. Energy diagram for zeolite-catalyzed alkene methylation with methanol: (1) Adsorption of methanol on the acidic site. (2) Coadsorption of the alkene in the vicinity of the methanol molecule. (3) Methylation. (4) Product desorption. The quantity measured experimentally is the apparent barrier, to which the appropriate heat of alkene adsorption (ΔH_{ads}) has to be added to get the intrinsic barrier.

method,[39,40] and on cluster models embedded in the full periodic ZSM-5, mordenite, and faujasite zeolite structures using the QM-Pot method.[32]

2. Experimental Data, and Assumptions about the Mechanism and the Catalyst Model

For the methylation of ethene, propene, and a thermodynamically equilibrated mixture of the three linear butene isomers (denoted *n*-butene) over H-ZSM-5, reaction rates and activation energies are known from experimental studies.[29,30] At experimental conditions (50 mbar methanol partial pressure, 13−50 mbar alkene partial pressure, 623 K reaction temperature), the methylation reactions were approximately first order with respect to the alkene and zero order with respect to methanol. That is, the measured Arrhenius activation barriers ($\Delta E^{\ddagger}$) of 109, 69, and 45 kJ/mol constitute apparent barriers with respect to the alkenes in the gas phase and to methanol adsorbed at the reaction site (see Figure 1). These values are related to the enthalpy of activation ($\Delta H^{\ddagger}$) according to eq 3.[41]

$$\Delta H^{\ddagger} = \Delta E^{\ddagger} - RT \tag{3}$$

Hence, the experimentally determined enthalpy barriers at 623 K are 104, 64, and 40 kJ/mol for the methylation of ethene, propene, and *n*-butene, respectively. Because the internal equilibration of the three linear butene isomers is significantly faster than the methylation reaction, *t*-2-butene as the thermodynamically most favored isomer is selected in the calculations representing *n*-butene.

We assume that the methylation occurs in a concerted way, that is, in a single step rather than in a two-step route involving a surface bound methoxy intermediate. Today, no definitive evidence in favor of either mechanism appears to exist, but there are indications from both theory and experiment that the concerted mechanism is the most likely. For the methylation of benzene and toluene (which may be considered relevant also for alkene methylation), Vos et al.[37] calculated a significantly higher barrier for the formation of the methoxy group than for the concerted methylation. Ivanova and Corma[42] studied the alkylation of toluene with methanol or dimethyl ether over H-ZSM-11 using in situ ^{13}C NMR. They concluded that concerted methylation was much faster than the coupling of a surface methoxy group with toluene. More recently, it was found that the methylation of propene over H-ZSM-5 proceeds much faster with dimethyl ether than with methanol.[43] If a methoxy intermediate were involved, the formation of this species would be rate determining, and no difference in the methylation rate would be expected across the various alkenes and aromatics, which is contradicted by the differences observed.[29,30]

Our calculations are made on the orthorhombic structure of ZSM-5, which is the high-temperature polymorph prevailing at reaction temperatures.[44−46] To create an acidic site, one of 96 Si atoms in the unit cell was replaced by an Al atom, resulting in a material with a Si/Al ratio of 95. In the experimental studies,[29,30] a catalyst with a Si/Al ratio of 45 was used. This corresponds to about two acidic sites per unit cell, which, however, are still well separated and can be considered as noninteracting. The orthorhombic H-ZSM-5 unit cell has 12 unique T-atom positions into which Al can be substituted. It is well beyond the scope of this study to perform an exhaustive investigation of all possible sites. Several computational studies have shown that there is little energetic preference for Al in different sites. Moreover, in a recent work, it is reported that the location of aluminum in ZSM-5 depends primarily on the synthesis conditions; that is, the Al distribution is kinetically controlled rather than thermodynamically.[47] In previous studies,[48,49] the Al7−O17(H)−Si4 "regular" site is considered the active site (see Figures S.2 and S.3) because it was found most stable in lattice energy minimizations using a classical shell model potential.[50] The Al12−O24(H)−Si12 "intersection" site is also of interest because of its location at the channel intersection with easy access for reactants and maximum reaction space. Clark et al.[32] considered the "intersection" site in their study of xylene disproportionation using the QM-Pot approach. As proton jumps between oxygen atoms bonded to the same aluminum are facile, in particular when an adsorbate is present,[27,51,52] the proton position for a given Al site is most likely determined by thermodynamics. In the present study, we also consider Al in the T12 site, but we find the proton more stable in the Al12−O20(H)−Si3 position (see further discussion in section S.2 of the Supporting Information).

3. Methods and Computational Details

Four different computational approaches have been pursued in this study. Stationary points on the potential energy surface of the methylation reaction pathway were first localized using DFT calculations on cluster models (see Supporting Information) to provide good starting structures for DFT calculations with periodic boundary conditions in which the entire H-ZSM-5 unit cell is taken into account. In single point calculations on structures obtained with the latter, both DFT-D and hybrid MP2:DFT have been used.

3.1. DFT with Periodic Boundary Conditions. The calculations were performed using the Vienna ab initio simulation package (VASP).[53−56] The projector-augmented wave (PAW) method[57] was

---

(39) Lesthaeghe, D.; De Sterck, B.; Van Speybroeck, V.; Marin, G. B.; Waroquier, M. *Angew. Chem., Int. Ed.* **2007**, *46*, 1311–1314.
(40) McCann, D. M.; Lesthaeghe, D.; Kletnieks, P. W.; Guenther, D. R.; Hayman, M. J.; Van Speybroeck, V.; Waroquier, M.; Haw, J. F. *Angew. Chem., Int. Ed.* **2008**, *47*, 5179–5182.
(41) Atkins, P. W. *Physical Chemistry*, 5th ed.; Oxford University Press: Oxford, 1994; pp 946−950.
(42) Ivanova, I. I.; Corma, A. *J. Phys. Chem. B* **1997**, *101*, 547–551.
(43) Svelle, S.; Kolboe, S.; Swang, O.; Olsbye, U. *J. Phys. Chem. B* **2005**, *109*, 12874–12878.
(44) Hay, D. G.; Jaeger, H.; West, G. W. *J. Phys. Chem.* **1985**, *89*, 1070–1072.
(45) van Koningsveld, H.; Jansen, H.; van Bekkum, H. *Zeolites* **1987**, *7*, 564–568.
(46) van Koningsveld, H. *Acta Crystallogr.* **1990**, *B46*, 731–735.
(47) Sklenak, S.; Dedecek, J.; Li, C.; Wichterlova, B.; Gabova, V.; Sierka, M.; Sauer, J. *Angew. Chem., Int. Ed.* **2007**, *46*, 7286–7289.
(48) Brändle, M.; Sauer, J. *J. Am. Chem. Soc.* **1998**, *120*, 1556–1570.
(49) Eichler, U.; Brändle, M.; Sauer, J. *J. Phys. Chem. B* **1997**, *101*, 10035–10050.
(50) Schröder, K.-P.; Sauer, J.; Leslie, M.; Catlow, C. R. A. *Zeolites* **1992**, *12*, 20–23.
(51) Sierka, M.; Sauer, J. *J. Phys. Chem. B* **2001**, *105*, 1603–1613.
(52) Franke, M. E.; Sierka, M.; Simon, U.; Sauer, J. *Phys. Chem. Chem. Phys.* **2002**, *4*, 5207–5216.
(53) Kresse, G.; Hafner, J. *Phys. Rev. B* **1993**, *48*, 13115–13126.
(54) Kresse, G.; Hafner, J. *Phys. Rev. B* **1994**, *49*, 14251–14269.
(55) Kresse, G.; Furthmüller, J. *Comput. Mater. Sci.* **1996**, *6*, 15–50.

employed in combination with the Perdew−Burke−Ernzerhof (PBE) exchange-correlation functional[58,59] and a 400 eV plane wave basis set kinetic energy cutoff value. Brillouin zone sampling was restricted to the Γ-point. Structures were considered converged when forces on all atoms were smaller than 0.05 eV/Å. For the largest system investigated in this work, the unit cell contains 307 atoms ($Si_{95}AlO_{193}C_5H_{13}$).

The H-ZSM-5 unit cell parameters were kept fixed in all calculations regarding the methylation reactions and location of the acidic site. To avoid any bias in favor of one specific aluminum and proton location, these parameters were determined for a completely siliceous material starting from crystallographic data. Relaxation of the ion positions for fixed cell parameters was first performed (300 eV kinetic energy cutoff). Subsequently, the lengths of the unit cell vectors were relaxed (800 eV kinetic energy cutoff). As mentioned, the orthorhombic symmetry of the unit cell was conserved throughout all calculations as no significant deviations are expected at relevant reaction temperatures.[44−46] The length of all three cell vectors increased: vector *a* from 20.022 to 20.157 Å, vector *b* from 19.899 to 20.033 Å, and vector *c* from 13.383 to 13.473 Å, which corresponds to an increase in unit cell volume from 5332 to 5441 Å^3.

Transition structures were located by judiciously transferring the active site structures determined with cluster model calculations (see section 1 of the Supporting Information) into the periodic environment and performing force minimizations using a quasi Newton algorithm.

To obtain zero-point vibrational energies (ZPVE) and finite temperature corrections required to calculate enthalpies, vibrational modes for the four periodic structures (adsorbed methanol and three transition structures) were calculated from numerical first derivatives of analytic atomic forces (step size 0.02 Å). Because of the extensive computational cost of these calculations (approximately 1800 energy evaluations for each of the four full systems), only a partial Hessian matrix was calculated for the evaluation of vibrational modes. The active space of this partial Hessian matrix covers the alkene and methanol molecules as well as 56 surrounding framework atoms (24 T-atoms including the Al atom plus 32 O atoms) that effectively encapsulate adsorbed or reacting molecules. Other framework atoms located farther from the active site occupy positions in space very similar in the reactant and the transition structures, and their contribution to the partition functions is likely to cancel out. This compromise reduces computational costs by about 75%. For molecules in the gas phase, the full Hessian was calculated.

3.2. DFT-D Calculations. Following Grimme,[20] the total energy of a system ($E_{\text{DFT-D}}$) is obtained by adding a semiempirical dispersion contribution (E_{disp}) to the self-consistent Kohn−Sham energy (E_{DFT}):

$$E_{\text{DFT-D}} = E_{\text{DFT}} + E_{\text{disp}} \tag{4}$$

with E_{disp} obtained by summing over damped C_6 terms for all atom pairs (N_{at} being the number of atoms),

$$E_{\text{disp}} = -s_6 \sum_{i=1}^{N_{\text{at}}-1} \sum_{j=i+1}^{N_{\text{at}}} \frac{\sqrt{C_6^i C_6^j}}{R_{ij}^6} f_{\text{damp}}(R_{ij}) \tag{5}$$

The s_6 parameter is a scaling factor unique for each functional (0.75 for PBE), f_{damp} is a damping function depending on the interatomic distance R_{ij}, and $C_6{}^i$ are atomic C_6 parameters all taken from ref 20.

3.3. Hybrid MP2:DFT Calculations. High-level corrections (eq 1) are evaluated as single point calculations on structures obtained with periodic model DFT. High-level structure relaxation effects are not expected to contribute significantly.[28] A series of 15 cluster models of increasing size was constructed for the adsorbed methanol structure (reference state, Figure 1) and all transition structures of the three methylation reactions, thus allowing the evaluation of apparent barrier heights. The cluster models were cut out from the periodic structure and saturated with hydrogen link atoms to avoid dangling bonds (r(AlO−H) = 0.953 Å, r(SiO−H) = 0.954 Å, r(Si−H) = 1.455 Å). To facilitate the calculations, Si−H rather than SiO−H termination was preferred with increasing model size. The cluster models are denoted as follows: 3T, 4T, $6T_{2H}$, $8T_{4H}$, $10T_{6H}$, $14T_{10H}$, $16T_{10H}$, $18T_{12H}$, $20T_{16H}$, $22T_{18H}$, $26T_{24H}$, $28T_{27H}$, $30T_{30H}$, $34T_{36H}$, and $38T_{42H}$, with the subscript indicating the number of Si−H terminations. Figure 2 shows the largest system investigated, the transition structure for the methylation of *t*-2-butene on the $38T_{42H}$ model with an overall composition $C_5H_{61}O_{59}Si_{37}Al$. For each cluster model and alkene molecule, MP2 energies were calculated with a TZVP basis set (see section 1 of the Supporting Information). Here, the “resolution-of-identity” (RI) integral approximation together with corresponding auxiliary basis sets[60] was employed as implemented in the “ricc2” module[61,62] of the Turbomole program.[63] Electrons from carbon 1s, oxygen 1s, aluminum 1s2s2p, and silicon 1s2s2p atomic orbitals were excluded from all electron correlation calculations in this work.

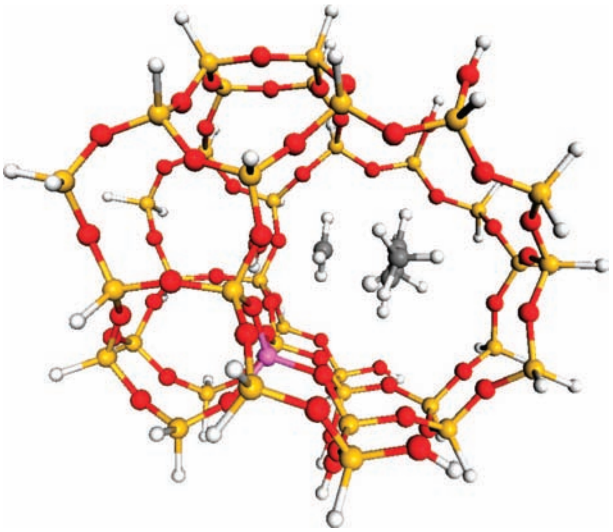

Figure 2. The largest system calculated with MP2/TZVP in this work is the $38T_{42H}$ cluster model transition structure for the methylation of *t*-2-butene (viewed along the straight channel; the zigzag channels run from left to right in the plane of the paper). The overall composition of the model is $C_5H_{61}O_{59}Si_{37}Al$. Color codes used: oxygen (red), silicon (yellow), aluminum (pink), hydrogen (white), carbon (gray).

The corresponding DFT energy calculations on these cluster models employ the same plane wave methodology used for the periodic structures to take advantage of the fact that plane waves do not introduce any basis set superposition error (BSSE). The dimensions of the computational box are defined individually for each cluster model size. That is, a cubic box was chosen large enough that distances between periodic images of the system are not smaller than 12 Å.[64] To ensure strict basis set consistency in calculated $\Delta E^{\ddagger}(\mathbf{C})_{\text{PBE}}$ values, for a given cluster model size barrier heights were obtained using the same box dimensions for each of the alkene molecules, the adsorbed methanol, and the transition structure.

---

(56) Kresse, G.; Furthmüller, J. *Phys. Rev. B* **1996**, *54*, 11169–11186.
(57) Blöchl, P. E. *Phys. Rev. B* **1994**, *50*, 17953–17979.
(58) Perdew, J. P.; Burke, K.; Ernzerhof, M. *Phys. Rev. Lett.* **1997**, *77*, 3865–3868.
(59) Perdew, J. P.; Burke, K.; Ernzerhof, M. *Phys. Rev. Lett.* **1997**, *78*, 1396–1396.
(60) Weigend, F.; Häser, M.; Patzelt, H.; Ahlrichs, R. *Chem. Phys. Lett.* **1998**, *294*, 143–152.
(61) Hättig, C.; Hellweg, A.; Köhn, A. *Phys. Chem. Chem. Phys.* **2006**, *8*, 1159–1169.
(62) Hättig, C. *J. Chem. Phys.* **2003**, *118*, 7751–7761.
(63) Ahlrichs, R.; Bär, M.; Häser, M.; Horn, H.; Kölmel, C. *Chem. Phys. Lett.* **1989**, *162*, 165–169.

Once $\Delta E^{\ddagger}(\mathbf{C}_n)_{\text{PBE}}$ and $\Delta E^{\ddagger}(\mathbf{C}_n)_{\text{MP2}}$ are known for the series of clusters $\mathbf{C}_n$, it is possible to obtain hybrid barriers composed of the periodic model DFT result and the high-level correction defined by eq 1,

$$\Delta E^{\ddagger}(\mathbf{S}{:}\mathbf{C}_n)_{\text{hybrid}} = \Delta E^{\ddagger}(\mathbf{S})_{\text{PBE}} + [\Delta E^{\ddagger}(\mathbf{C}_n)_{\text{MP2}} - \Delta E^{\ddagger}(\mathbf{C}_n)_{\text{PBE}}] \qquad (6)$$

A key step in the hybrid MP2:DFT approach is to extrapolate the high-level corrections to the barrier height obtained for finite size cluster models, $\Delta E^{\ddagger}(\mathbf{C}_n)_{\text{high}}$, to the periodic model limit. This extrapolation procedure has been described in detail previously.[28] Briefly, an analytical expression is required capable of reproducing $\Delta E^{\ddagger}(\mathbf{C}_n)_{\text{high}} = \Delta E^{\ddagger}(\mathbf{C}_n)_{\text{MP2}} - \Delta E^{\ddagger}(\mathbf{C}_n)_{\text{PBE}}$ for each cluster model size n. The damped dispersion atom−atom pair expansion given in eq 5 constitutes the first of two terms in this analytical expression. We have not restricted atom−atom interactions to specific fragments within our systems; all atom−atom interactions are included. The scaling factor s_6 is not explicitly considered, that is, $s_6 = 1$. The second term in the analytical expression is an additive constant E_{add} accounting for all effects contributing to MP2-PBE differences not related to long-range dispersion, for example, for self-interaction errors. Fitting the high-level correction term is achieved by minimizing.

$$\Delta(\{C_6^i\}, E_{\text{add}}) = \sum_{n=1}^{n_{\max}} [\Delta E^{\ddagger}(\mathbf{C}_n)_{\text{MP2}} - \Delta E^{\ddagger}(\mathbf{C}_n)_{\text{PBE}} - (\Delta E^{\ddagger}(\mathbf{C}_n)_{\text{C6}} + E_{\text{add}})]^2 \qquad (7)$$

For each of the three methylation reactions, $\{C_6{}^i\}$ and E_{add} were fitted individually using a series of $n_{\max}$ cluster model sizes. Analytic partial first derivatives of Δ with respect to the parameters $(\{C_6^i\}, E_{\text{add}})$ and standard numerical procedures were employed for fitting. No constraints were applied for E_{add}, whereas all atomic $C_6{}^i$ parameters were restricted to positive values. The latter is important to ensure proper convergence behavior of $E(\mathbf{C}_n)_{\text{C6}}$ with growing size of the cluster model up to the periodic limit (lattice sum). The physical meaning of the C_6 parameters derived from fitting is limited, and they are certainly not transferable to other systems. Employing fitted C_6 parameters, $\Delta E^{\ddagger}(\mathbf{S})_{\text{C6}}$ is obtained by applying eq 5 to the periodic structures (involving the calculation of lattice sums)[24] and to the gas-phase alkene molecule. Adding E_{add} yields an estimate for the high-level correction of the full periodic structure ($\mathbf{S}$):

$$\Delta E^{\ddagger}(\mathbf{S})_{\text{high}} = \Delta E^{\ddagger}(\mathbf{S})_{\text{MP2}} - \Delta E^{\ddagger}(\mathbf{S})_{\text{PBE}} \approx \Delta E^{\ddagger}(\mathbf{S})_{\text{C6}} + E_{\text{add}} \qquad (8)$$

Adding this term to the corresponding DFT barriers, $\Delta E^{\ddagger}(\mathbf{S})_{\text{PBE}}$ obtained in section 4.2 yields estimates for full periodic model MP2 barrier heights (cf., eq 2).

3.4. Complete Basis Set Extrapolation. MP2 results are affected by errors due to the incompleteness of Gaussian basis sets. To assess this error and its model size dependency, for the seven smallest cluster models (3T−16T$_{10\text{H}}$) additional MP2 calculations have been performed using Dunning's correlation consistent polarized valence triple- and quadruple-ζ basis sets (cc-pVTZ and cc-pVQZ).[65,66] Extrapolation to the complete basis set (CBS) limit assumes an exponential behavior of the Hartree−Fock energy and an X^{-3} behavior of the correlation energy as a function of the basis set cardinal number X (=3,4). For the smallest cluster model (3T), explicitly correlated MP2-F12 reference calculations[67] were performed to ensure that the MP2 CBS limit extrapolation yields reliable results. The full procedure is described in section 3 of the Supporting Information.

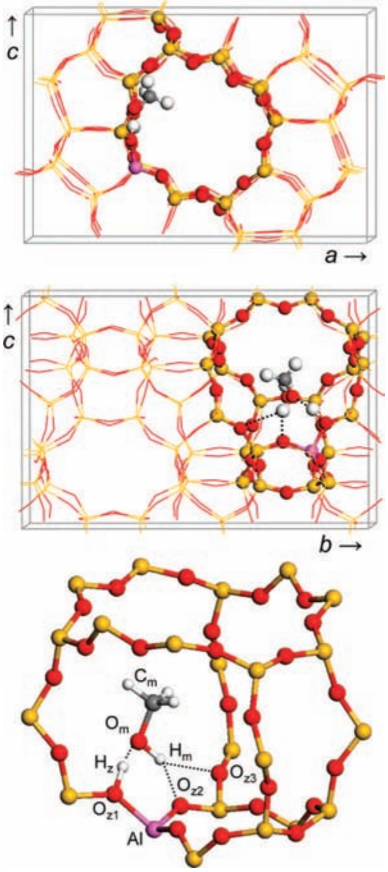

Figure 3. Methanol adsorbed in zeolite H-ZSM-5: unit cell view along the straight channels in the b direction (top panel), the sinusoidal channels in the a direction (middle panel). Highlighted atoms (enlarged in bottom panel) define the intersection between the channels. The methanol molecule interacts with the framework via two hydrogen bonds and is located in the plane of a 10-membered ring defined by the sinusoidal channel. Crystallographic atom numbering: Al = Al12 and O$_{z1}$ = O20 and O$_{z2}$ = O24.

3.5. Electron Correlation beyond MP2. The ability of MP2 to reproduce barrier heights for methylation reactions in zeolites reliably was assessed by performing single point coupled-cluster calculations including single, double, and perturbatively treated connected triple excitations (CCSD(T)) using the MOLPRO code.[68] Because of high computational expenses, only the 3T cluster models were considered employing the TZVP basis set.

4. Results and Discussion

4.1. Adsorption of Methanol and Coadsorption of Alkenes. Periodic model PBE and PBE-D calculations have been performed for the adsorption of methanol in H-ZSM-5 and the coadsorption of the alkenes in methanol loaded H-ZSM-5.

4.1.1. Adsorption of Methanol. The energy minimum structure for adsorbed methanol is shown in Figure 3, and geometric

---

(64) To verify that the interaction between periodic images can be neglected this way, a series of 3T cluster model test calculations was performed employing a computational box doubled in one direction containing the original system and an inverted replica in the appropriate distance. The resulting apparent barrier heights did not differ by more than 1 kJ/mol from the values obtained with a cubic box containing only the original system.

(65) Dunning, T. H., Jr *J. Chem. Phys.* **1989**, *90*, 1007–1023.

(66) Woon, D. E.; Dunning, T. H., Jr *J. Chem. Phys.* **1993**, *98*, 1358–1371.

(67) Klopper, W.; Manby, F. R.; Ten-No, S.; Valeev, E. F. *Int. Rev. Phys. Chem.* **2006**, *25*, 427–468.

(68) Werner, et al.; *MOLPRO−a package of ab initio programs (version 2002.6)*; Birmingham, UK, 2003.

Table 1. Atomic Distances (in Å) for Relaxed Periodic Model Structures (PBE)[a]

	adsorbed methanol	transition structure for methylation of		
		ethane	propene	*t*-2-butene
$O_{z1}H_z$	1.11	1.84	1.77	1.77
$O_{z2}H_m$	1.79	1.98	2.08	2.18
$O_{z3}H_m$	2.65	2.66	2.59	2.61
H_zO_m	1.36	0.99	1.00	1.00
H_mO_m	1.00	0.99	0.99	0.98
O_mC_m	1.45	2.18	2.09	2.06
C_mC_{a1}	N/A	2.16	2.15	2.34
C_mC_{a2}	N/A	2.21	2.44	2.30

[a] Atom labels are defined in Figures 3−5.

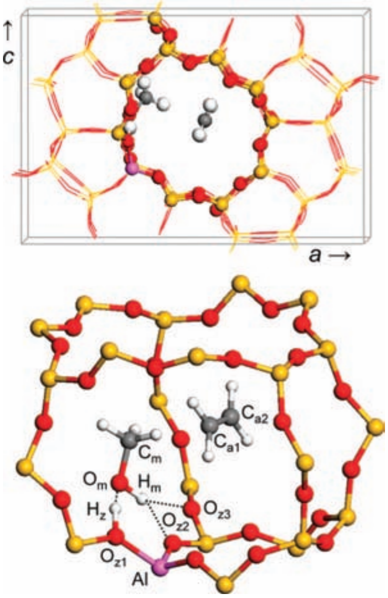

Figure 4. Coadsorbed methanol and ethene in zeolite H-ZSM-5: unit cell view along the straight channels in the *b* direction (top panel).The alkene resides in the center of the straight channels with no specific interactions with the methanol molecule or the zeolite wall.

parameters are listed in Table 1. Atom labels defined in Figures 3−5 will also be used in the following. The adsorption mode found for the periodic model is very similar to the one obtained by DFT calculations on cluster models (see Supporting Information). Methanol is adsorbed end-on forming two hydrogen bonds, a strong one between the acidic proton (H_z) and the methanol oxygen (O_m) and another between the methanol hydroxyl proton (H_m) and a zeolite oxygen (O_{z2}). The distance between the methanol proton and a second zeolite oxygen (O_{z3}) is outside the hydrogen bond range (2.65 Å). This configuration is similar to that described by Haase and Sauer[69] in a periodic model DFT study of methanol adsorption at the Al7−O17(H)−Si4 “regular” H-ZSM-5 acidic site. The methanol adsorption energy is −86 kJ/mol in comparison to −77 kJ/mol (PBE/TZVP) for the cluster model and to −88 kJ/mol for methanol adsorption in zeolite mordenite (periodic model).[36]

When the geometry optimization for adsorbed methanol was started with the acidic proton at the Al12−O24(H)−Si12 “intersection” site, which is 12 kJ/mol less stable and therefore more prone to proton transfer, a different stationary point was located. In this case, the methanol becomes protonated with two equally long O_m−hydrogen distances and two very similar hydrogen bonds to the zeolite framework. The adsorption energy of −89 kJ/mol is virtually indistinguishable from the value found for the stationary point discussed above. A partial Hessian calculation suggested that an energy minimum rather than a transition structure for proton jump between two zeolite oxygen atoms (O−Al−O) was found. A short microcanonical molecular dynamics simulation resulted in the immediate return of a proton to its most stable location (O20). Also, whether or not methanol exists as a protonated species has been examined for H-ZSM-5[69] and H-chabazite,[70,71] and the results clearly indicate that methanol is not protonated. Therefore, in this study, reference is made to the nonprotonated methanol structure depicted in Figure 3.

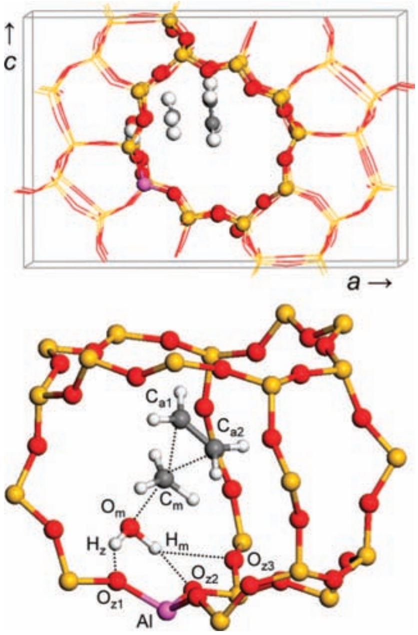

Figure 5. Transition structure for the methylation of ethene in zeolite H-ZSM-5: unit cell view along the straight channels in the *b* direction (top panel). The water molecule forms hydrogen bonds with zeolite oxygen atoms, and the methyl cation and the alkene molecule are directed into the channel intersection.

4.1.2. Coadsorption of the Alkene. To obtain apparent barriers, the stationary points on the potential energy surface for the coadsorption of the alkenes are not required. Nevertheless, they will be briefly discussed because they illustrate the inability of the applied density functionals to account for dispersive interactions. Figure 4 shows the structures obtained for coadsorbed methanol and ethene. All alkenes are located in the center of the straight channels, as they are not involved in any specific interactions with the methanol molecule or the zeolite. For ethene, the closest contact (2.70 Å) is between a methanol hydrogen atom and an ethene carbon atom. Similar minimum structures were obtained for propene and *t*-2-butene. Table 2 lists the adsorption energies, which are all very small (about −10 kJ/mol), and there is no trend with respect to the alkene size. When ethene is placed in a very similar position with adsorbed methanol in a straight channel not containing an acidic site, that is, in a pure silica form, the alkene adsorption energy is reduced by only ~2 kJ/mol. This confirms that there is no or

---

(69) Haase, F.; Sauer, J. *Microporous Mesoporous Mater.* **2000**, *35−36*, 379–385.

(70) Shah, R.; Gale, J. D.; Payne, M. C. *J. Phys. Chem.* **1996**, *100*, 11688–11697.

(71) Haase, F.; Sauer, J.; Hutter, J. *Chem. Phys. Lett.* **1997**, *266*, 397–402.

Table 2. Energy Values (kJ/mol) for the Adsorption of Methanol and the Coadsorption and Methylation of the Alkenes in H-ZSM-5 Calculated for Periodic Models by PBE and PBE-D

	methanol	ethene	propene	*t*-2-butene
Adsorption Energy				
periodic model PBE	−86	−10	−11	−9
periodic model PBE-D	−115	−37	−53	−68
experiment	−115 ± 5[a]	−24 to −31[b]	−40[b]	−49[b,c]
Methylation Reaction Apparent Barrier				
4T cluster model PBE (B3LYP)		164 (197)	147 (177)	142 (171)
periodic model PBE		109	89	86
periodic model PBE-D		75	40	12
experiment[d]		94	54	30

[a] Enthalpy, see ref 73. [b] Available enthalpies for alkenes in silicalites, see ref 74 and references therein. [c] Experimental value for 1-butene. [d] Estimated from experimental enthalpies (refs 29 and 30) by subtracting ZPVE and finite temperature corrections obtained from periodic model PBE partial Hessian calculations.

Table 3. Hybrid MP2:PBE Apparent Barriers for the Methylation of the Alkenes in H-ZSM-5 and Decomposition into Their Different Energy Contributions (kJ/mol)[a]

	model	alkene		
		ethene	propene	*t*-2-butene
$\Delta E^{\ddagger}(\mathbf{C})_{\mathrm{MP2}}$	3T	195	170	125
$\Delta E^{\ddagger}(\mathbf{C})_{\mathrm{PBE}}$		172	149	123
$\Delta E^{\ddagger}(\mathbf{C})_{\mathrm{MP2}} - \Delta E^{\ddagger}(\mathbf{C})_{\mathrm{PBE}}$		22	21	2
$\Delta E^{\ddagger}(\mathbf{S{:}C})_{\mathrm{hybrid}}$		131	111	88
$\Delta E^{\ddagger}(\mathbf{C})_{\mathrm{MP2}}$	$38\mathrm{T}_{42\mathrm{H}}$	125	99	66
$\Delta E^{\ddagger}(\mathbf{C})_{\mathrm{PBE}}$		127	109	103
$\Delta E^{\ddagger}(\mathbf{C})_{\mathrm{MP2}} - \Delta E^{\ddagger}(\mathbf{C})_{\mathrm{PBE}}$		−2	−10	−37
$\Delta E^{\ddagger}(\mathbf{S{:}C})_{\mathrm{hybrid}}$		107	80	49
$\Delta E^{\ddagger}(\mathbf{S})_{\mathrm{MP2}}$[b]	periodic	102	74	43
$\Delta E^{\ddagger}(\mathbf{S})_{\mathrm{PBE}}$		109	89	86
$\Delta E^{\ddagger}(\mathbf{S})_{\mathrm{MP2}} - \Delta E^{\ddagger}(\mathbf{S})_{\mathrm{PBE}}$[c]		−7	−15	−43

[a] MP2 results are obtained with the TZVP basis set. [b] Estimate, obtained by adding $\Delta E^{\ddagger}(\mathbf{S})_{\mathrm{PBE}}$ to the results of the last line (eq 2). [c] High-level correction, calculated from fitted data as "$\Delta E^{\ddagger}(\mathbf{S})_{\mathrm{C6}} + E_{\mathrm{add}}$" (eqs 7 and 8).

very little specific interaction between the alkenes and the methanol/acidic site. This underestimation of adsorption energies is one major reason why DFT (PBE) does not reproduce experimentally observed apparent barrier heights (vide infra).[33,72]

4.1.3. DFT-D Results and Comparison with Experiment. Table 2 shows the results of DFT-D single point calculations for periodic model DFT structures as defined by eqs 4 and 5. Adding dispersion results in a stronger binding of the methanol molecule, by as much as −29 kJ/mol, and a very good match is obtained with the experimental adsorption enthalpy[73] of −115 ± 5 kJ/mol (H-ZSM-5, Si/Al = 26). The latter value is obtained by microcalorimetry for loadings below one molecule per site, and there is little variation of this value as a function of loading as expected for adsorption on isolated sites.

Also, for the coadsorbed alkenes, DFT-D yields adsorption energies that are larger and show the expected increase with growing alkene chain length. Experimental heats of adsorption for alkenes in acidic H-ZSM-5 are not available, but Jakobtorweihen et al.[74] have compiled all available experimental data for alkenes in silicalite-1, the aluminum free H-ZSM-5 analogue. These results are included in Table 2 and may be suitable for comparison, because in the present coadsorption case the alkene is not interacting with the acidic site but rather with the surrounding zeolite wall and the methanol molecule. Although somewhat on the large side, Table 2 shows that the PBE-D values a substantial improvement as compared to periodic PBE. It should also be kept in mind that we are comparing calculated electronic energies with experimental enthalpies.

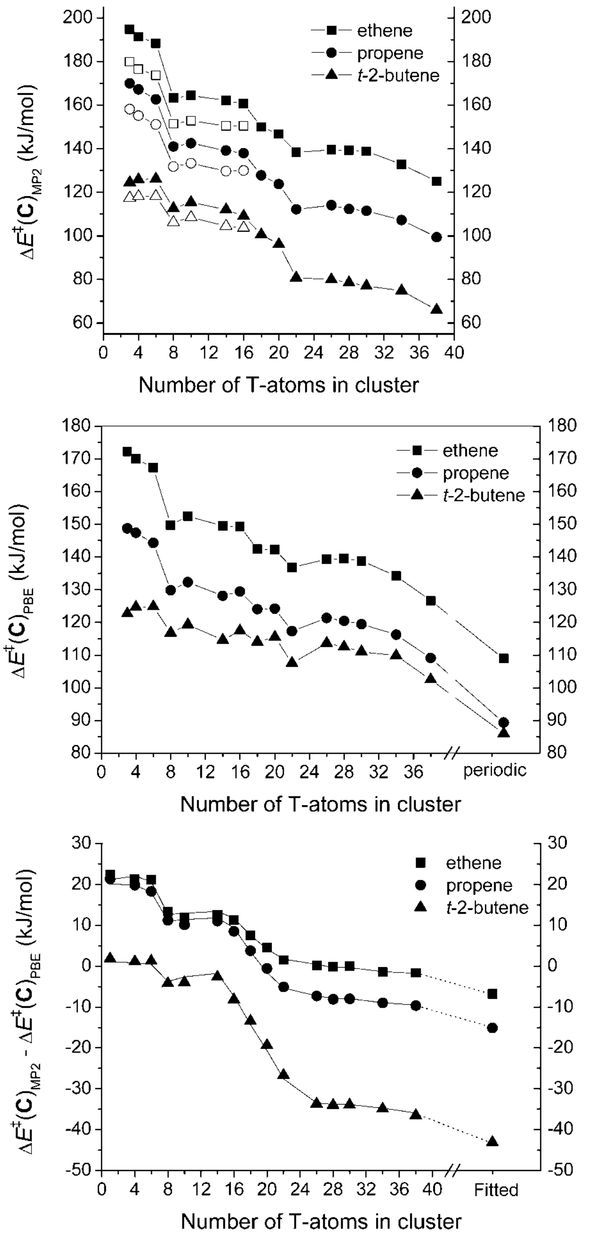

Figure 6. Apparent barriers for alkene methylation obtained from single point calculations on structure models of increasing size. Top panel: MP2/TZVP (filled symbols) and MP2/CBS limit results (open symbols). Middle panel: DFT (PBE) results. The periodic model reference is included for comparison. Bottom panel: Difference between the two series ($\Delta E^{\ddagger}(\mathbf{C})_{\mathrm{MP2}} - \Delta E^{\ddagger}(\mathbf{C})_{\mathrm{PBE}}$) representing the high-level correction to periodic model DFT results (eqs 1 and 8).

4.2. Methylation Reactions.

4.2.1. 4T Cluster Model Calculations. Calculations on 4T cluster models were carried out using both PBE/TZVP and B3LYP/TZVP. Table 2 shows the apparent energy barriers. Similar to previous cluster model studies,[35,37] they are 70−112

---

(72) Van Santen, R. A.; Rozanska, X. *Adv. Chem. Eng.* **2001**, *28*, 399–436.

(73) Lee, C.-C.; Gorte, R. J.; Farneth, W. E. *J. Phys. Chem. B* **1997**, *101*, 3811–3817.

(74) Jakobtorweihen, S.; Hansen, N.; Keil, F. J. *Mol. Phys.* **2005**, *103*, 471–489.

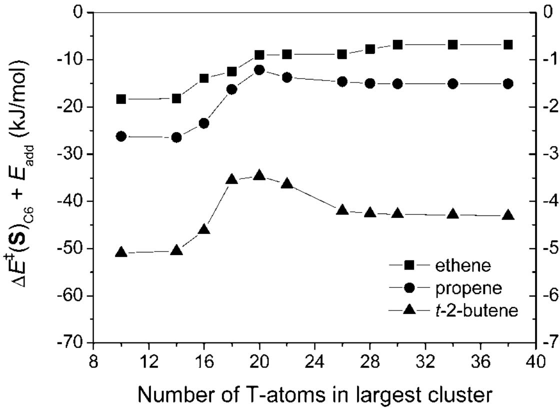

Figure 7. Extrapolated values for the periodic model high-level correction to the apparent barriers ($\Delta E^{\ddagger}(\mathbf{S})_{MP2} - \Delta E^{\ddagger}(\mathbf{S})_{PBE}$) as a function of the largest cluster model included in the fitting procedure.

(PBE) and 103−141 kJ/mol (B3LYP) higher than experimental barriers (Table 2, see also Supporting Information).

4.2.2. Periodic Model PBE Calculations. The transition structure for the methylation of ethene is shown in Figure 5, and geometric parameters are listed in Table 1. For all three alkenes, the transition structures are very similar to those obtained in 4T cluster model calculations (Supporting Information, Table S1): A water molecule is formed, and the methyl cation is located between that water molecule and the alkene double bond. The only significant difference is that one of the hydrogen bonds between water and the zeolite wall ($O_{z2}H_m$) is longer when studied under periodic boundary conditions.

Table 2 shows our periodic PBE results for apparent barriers in comparison to "experimental energy barriers", which have been derived from experimentally determined enthalpies of activation at 623 K (104, 64, and 40 kJ/mol for the methylation of ethene, propene, and *n*-butene, respectively) by subtracting ZPVE and finite temperature corrections (periodic model PBE results, see section 4.2.3). For the methylation of ethene, the calculated apparent barrier is 15 kJ/mol larger than the experimental value (Table 2), and the difference between DFT (PBE) and experiment becomes larger for propene (45 kJ/mol) and even larger for *t*-2-butene (56 kJ/mol). These observations can be rationalized by assuming that for ethene the two major errors of GGA-type functionals, missing dispersion contributions and the tendency to underestimate barrier heights, to a large degree cancel out, whereas for propene and *t*-2-butene the growing dispersion contribution is no longer compensated by a more or less constant self-interaction error on the barrier height.

This effect is clearly seen after the damped dispersion term is added to the PBE results (eqs 4 and 5). For all three alkenes, apparent barriers are uniformly underestimated by 14−19 kJ/mol (Table 2). This underestimation is typical for GGA-type functionals in general and PBE in particular, as evidenced by benchmark results of ref 15. Hence, DFT-D provides a significant improvement as compared to DFT results, but with hybrid MP2:DFT calculations reported in section 4.2.4, a further improvement is achieved.

4.2.3. Zero-Point Energy and Enthalpy Corrections from Periodic DFT. For adsorbed methanol and the transition structures, partial Hessian matrices were calculated. For the reactants, no negative Hessian eigenvalues were found, and exactly one negative eigenvalue was obtained for the transition structures. ZPVE corrections shift the barriers slightly by +5.1, +3.7, and +3.7 kJ/mol for the methylation of ethene, propene, and *t*-2-butene, respectively. Finite temperature corrections at 623 K (experimental temperature) lead to additional shifts by +5.0, +6.4, and +6.6 kJ/mol, respectively. Hence, for all barriers, a uniform increment of +10 kJ/mol transforms total energies into enthalpies. PBE calculations on 4T cluster models (Supporting Information, Table S.2) yield smaller ZPVE contributions to the barriers (not exceeding 1 kJ/mol), whereas finite temperature corrections agree fairly well. For B3LYP, however, the results appear to be less consistent within the series of alkenes.

4.2.4. Hybrid MP2:DFT Calculations. Table 3 shows the various contributions to the hybrid MP2:PBE apparent barrier heights according to eq 6 for the smallest and the largest cluster models. The effects of the cluster size is substantial. For the smallest model (3T), the barriers are higher with MP2 than with PBE, whereas this order is reversed for the largest model ($38T_{42H}$). The dependence on cluster size is also shown in Figure 6. MP2 barriers for the methylation of ethene and propene fall steeply with increasing cluster size up to the $22T_{18H}$ model, whereas for *t*-2-butene the barrier is fairly stable for small clusters, but drops substantially for larger ones. Beyond the $22T_{18H}$ cluster, the effects of cluster size are less pronounced, and the barriers for all three methylation reactions decrease more slowly. Note that the barriers decrease by as much as 59−70 kJ/mol throughout the MP2 series, whereas with PBE these changes are smaller, 20−46 kJ/mol. This shows, first, that any attempt of deriving accurate results from plain cluster model calculations requires huge cluster sizes. Even for the largest model, PBE barriers are still 17−20 kJ/mol above the periodic limit. Second, the long-range part of the dispersive interaction between the zeolite and the reactants is missing with PBE, as indicated by the steeper decrease of the $\Delta E^{\ddagger}(\mathbf{C})_{MP2}$ series. This observation still holds when effects due to MP2 basis set incompleteness are considered (see below). For both MP2 and PBE, the relative order of the barrier heights for the alkene series is the same for all model sizes considered.

Figure 7 illustrates the stability of the fitting procedure with respect to the number n_{max} of cluster models of increasing size included in the fit (eq 7). It shows the high-level correction, $\Delta E^{\ddagger}(\mathbf{S})_{C6} + E_{add}$, evaluated with parameters $\{C_6^i\}$ and E_{add} obtained from fits to data sets of increasing size (n_{max}). The smallest data set, $n_{max} = 5$, includes the five smallest models up to size $10T_{6H}$, whereas the largest data set covers all model sizes ($n_{max} = 15$). Figure 7 shows that convergence is achieved when the largest cluster included in the fit corresponds to at least the $28T_{27H}$ model ($n_{max} = 12$). Inclusion of more (and larger) cluster models changes the periodic limit by less than 1 kJ/mol. When all reference data points are included for fitting ($n_{max} = 15$), root mean squared errors (maximum errors) between reference data points and corresponding fitted values are 0.6 (−1.3), 0.6 (1.3), and 0.8 (1.4) kJ/mol for ethene, propene, and *t*-2-butene, respectively. This implies an error bar of ±2 kJ/mol for the periodic model limits of the high-level corrections, $\Delta E^{\ddagger}(\mathbf{S})_{MP2} - \Delta E^{\ddagger}(\mathbf{S})_{PBE}$, which are −7, −15, and −43 kJ/mol for the methylation of ethene, propene, and *t*-2-butene, respectively.

4.2.5. Basis Set Superposition Error and Complete Basis Set Limit. BSSE corrections and CBS limit extrapolations have been performed for the MP2 apparent barrier heights of the seven smallest cluster models ($3T-16T_{10H}$). Table 4 shows the results for the $16T_{10H}$ cluster model. The BSSE on the barrier heights is 10−25% with the cc-pVTZ basis set and still 4−10% with cc-pVQZ. This is the result of some compensation between

Table 4. Basis Set Dependency of Cluster Model MP2 Apparent Barriers for the Methylation of the Alkenes, and CBS Limit Extrapolations[a]

			apparent barrier heights for the methylation of					
basis set	model	component	ethene		propene		*t*-2-butene	
TZVP	$16T_{10H}$	HF	188		178		164	
		MP2 (correl.)	−27		−40		−55	
		MP2 (total)	161		138		109	
cc-pVTZ	$16T_{10H}$	HF	189	(196)	178	(187)	163	(174)
		MP2 (correl.)	−32	(−25)	−47	(−37)	−61	(−48)
		MP2 (total)	156	(171)	132	(151)	102	(126)
cc-pVQZ	$16T_{10H}$	HF	190	(192)	181	(184)	167	(170)
		MP2 (correl.)	−38	(−34)	−51	(−46)	−64	(−58)
		MP2 (total)	152	(158)	130	(138)	102	(112)
CBS limit	$16T_{10H}$	HF	191		183		170	
		MP2 (correl.)	−41		−53		−66	
		MP2 (total)	150		130		104	
CBS limit	3T	HF	213		201		173	
		MP2 (correl.)	−33		−43		−55	
cc-pV5Z	3T	HF	212	(213)	200	(201)	172	(172)
aug-cc-pVTZ	3T	MP2-F12 (correl.)	−33		−44		−56	

[a] Values in parentheses are corrected for the BSSE (kJ/mol).

Table 5. Correlation Energy Contributions to Apparent Barriers for the Methylation of the Alkenes Calculated for 3T Cluster Models Using the TZVP Basis Set (kJ/mol)

	apparent barriers for the methylation of		
	ethene	propene	*t*-2-butene
RI-MP2 (correl.)	−19.6	−30.2	−44.9
MP2 (correl.)	−19.4	−30.0	−44.6
CCSD(T) (correl.)	−17.3	−29.8	−44.5

Table 6. Final Estimates of Apparent Barriers for the Methylation of the Alkenes in H-ZSM-5 and Comparison with Experiment (kJ/mol)

	apparent barriers for the methylation of		
	ethene	propene	*t*-2-butene
periodic model DFT (PBE)	108.9	89.3	86.0
increment from corrections for			
MP2/TZVP − PBE (periodic model limit)	−6.8	−15.1	−43.1
MP2/CBS − MP2/TZVP ($16T_{10H}$ cluster model)	−10.3	−7.9	−5.4
CCSD(T) − MP2 (3T cluster model)	+2.2	+0.4	+0.4
final energy barrier	94.0	66.7	37.9
ZPVE correction[a]	+5.1	+3.7	+3.7
finite temperature correction[a] (623 K)	+5.0	+6.4	+6.6
final enthalpy barrier (623 K)	104	77	48
experimental enthalpy barrier (623 K)	104	64	40

[a] From DFT (PBE) frequency calculations.

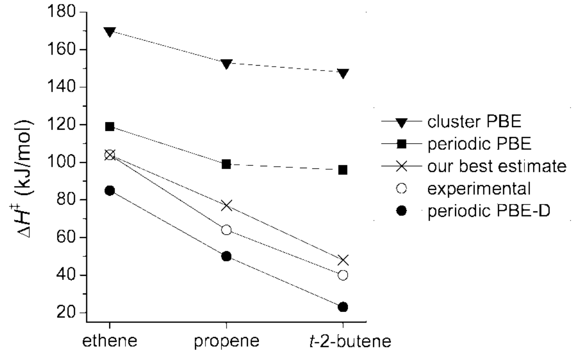

Figure 8. Apparent enthalpy barriers for the methylation of three alkenes obtained with various computational schemes as compared to experimental data (see text).

the BSSE for the reference structure (adsorbed methanol) of −24 (−10) kJ/mol and the BSSE for the transition structures for ethene, propene, and *t*-2-butene, −39 (−17), −43 (−18), and −48 (−21) kJ/mol, respectively (cc-pVTZ results, cc-pVQZ results in parentheses).

Table 4 also lists results for the smallest, 3T cluster model. It is sufficiently small so that more advanced reference calculations can be performed to check if the CBS limit extrapolation of BSSE corrected barrier heights yields reliable results (the decomposition of the structures for BSSE calculations is not unique). For the HF part, the quintuple-zeta basis set (cc-pV5Z) used yields results within 1 kJ/mol of the extrapolated CBS limits. MP2 correlation energies, however, converge much slower with extending the basis sets, rendering MP2 calculations with virtually complete basis sets practically impossible, unless explicitly correlated MP2 calculations are made. Our MP2-F12 results (Table 4, last row) agree within 1 kJ/mol with the CBS extrapolated MP2 correlation energies.

After having assured ourselves that the MP2/CBS results from BSSE corrected MP2 energies are reliable, we compare them for the $16T_{10H}$ models with barrier heights obtained by our standard MP2/TZVP calculations (top rows of Table 4). We find that the latter do remarkably well, which is due to extensive cancelation of basis set superposition and basis set incompleteness errors in MP2/TZVP calculations. The differences are −10, −8, and −5 kJ/mol for the methylation of ethene, propene, and *t*-2-butene, respectively. Obviously, the larger is the hydrocarbon, the smaller is the error due to basis set truncation.

As our primary interest is to extrapolate MP2/TZVP barrier heights to their periodic model limit, we consider the differences between MP2/CBS and MP2/TZVP results as a function of cluster size. For the seven smallest cluster models (3T, 4T, $6T_{2H}$, $8T_{4H}$, $10T_{6H}$, $14T_{10H}$, $16T_{10H}$), Figure 6 (top panel) shows that the MP2/CBS data (open symbols) follow the trend of MP2/TZVP results (filled symbols). For the methylation of ethene, propene, and *t*-2-butene, the difference varies throughout the $3T-16T_{10H}$ series within a range of 5, 4, and 3 kJ/mol, respectively, with a slight tendency to smaller differences with increasing cluster size. Nevertheless, we assume that this difference remains constant beyond $16T_{10H}$ and use the above $16T_{10H}$ results, that is, −10, −8, and −5 kJ/mol for the methylation of ethene, propene, and *t*-2-butene, respectively, as MP2 CBS limit corrections also for the periodic limit of the MP2/TZVP barrier heights.

4.2.6. Correlation Energies beyond MP2. The CCSD(T)/TZVP apparent barriers calculated for the 3T cluster model are listed in Table 5. Canonical MP2 results obtained along CCSD(T) calculations are included and show that the error due to the RI approach is negligible in the RI-MP2 calculations of this work. For the methylation of propene and *t*-2-butene, the difference between CCSD(T) and RI-MP2 is very small (+0.4 kJ/mol), whereas for the methylation of ethene a slightly larger CCSD(T)-RI-MP2 correction is obtained (+2.2 kJ/mol). These differences between RI-MP2 and CCSD(T) are in line with what was seen in a previous study on iso-butene adsorption in H-Ferrierite,[28] and it is concluded that in the present work RI-MP2 yields energy barriers of chemical accuracy. Nevertheless, for the final estimates, the CCSD(T)-RI-MP2 corrections will be included. It seems that in comparison to the larger alkenes the methylation of ethene is slightly more demanding for ab initio electronic structure modeling. A similar observation was made for the CBS limit extrapolation of the MP2 barrier heights (see Table 4).

4.3. Final Estimates − Comparison with Experiment. Table 6 summarizes all of the contributions leading to our final estimates for the enthalpy barriers of alkene methylation reactions in zeolite H-ZSM-5. The deviations between our best estimates and experiment are 0, 13, and 8 kJ/mol for the methylation of ethene, propene, and *t*-2-butene, respectively. Such comparison is affected by uncertainties in both the theoretical and the experimental results that are difficult to assess. Inspection of the Arrhenius plots in refs 29 and 30 reveals significant and systematic deviations from linearity, that is, from strict Arrhenius behavior. This may be caused by minor variations in the reaction orders throughout the investigated temperature ranges and by non-negligible conversions of reactants (and thus any side reactions) for some data points, in particular those measured at high temperature. For example, the Arrhenius activation energy for the methylation of ethene (109 kJ/mol) is obtained in ref 29 as the average of two values, 103 and 114 kJ/mol, which implies an uncertainty of at least ±5 kJ/mol.

With respect to the calculated data, it was shown above that the fitting procedure results in an uncertainty of ±2 kJ/mol for the periodic limit value of the high-level correction. Together with the variation of the CBS estimate for the MP2 energy (up to ±2.5 kJ/mol), this results in a minimum uncertainty of about ±5 kJ/mol. Additional uncertainty is connected with the choice of the reference cell (here optimized for pure silica), the level at which the atomic positions are optimized (in this study periodic model PBE instead of hybrid MP2:PBE), and the location of the active site in the zeolite framework. Similarly to a previous study,[28] a range of ±10 kJ/mol is assumed to account for all uncertainties, which means that calculated and experimental data agree within the associated errors.

5. Conclusions

The hybrid MP2:DFT method presented here reproduces reaction barriers for the methylation of alkenes in the presence of zeolite catalysts with near chemical accuracy (deviations between 0 and 13 kJ/mol). This is a significant improvement as compared to periodic model PBE results, which show much larger deviations from experiment and fail to reproduce the decrease in the ethene, propene, *t*-2-butene series; see Figure 8. This can be partly rectified when augmenting DFT with a semiempirical dispersion term (PBE-D), but the barriers still remain systematically too low (by 14−19 kJ/mol), as is typical for this type of functionals.

Whereas predictions of activation enthalpies with near chemical accuracy by local electron correlation methods in hybrid QM:MM calculations have already been reported for well-characterized enzymes,[75] the present results show that this is possible also for individual steps of hydrocarbon synthesis and conversion reactions in zeolites. With this, substantial progress has been made toward the simulation of complex reaction networks in zeolites such as the hydrocarbon pool mechanism. The next task is getting pre-exponentials with the same accuracy. This is a challenge because the harmonic approximation faces its limits at temperatures as high as needed for hydrocarbon conversion in zeolites, and available sampling techniques require high-quality force fields that are not yet available for zeolites with reaction sites.

Acknowledgment. This work has been supported by the Cluster of Excellence “Unifying Concepts in Catalysis” and by the German Research Foundation (Priority Programme 1155). We also thank the Norddeutscher Verbund für Hoch- and Höchstleistungsrechner (HLRN) for computing time and the Research Council of Norway for a grant of computer time through the NOTUR project (account NN2878K). For the RI-MP2-F12 calculations, we have received indispensable support from Sebastian Hoefener in the group of Wim Klopper (Universität Karlsruhe).

Supporting Information Available: Description of DFT calculations on cluster models; discussion of possible locations of the acidic site in H-ZSM-5; complete description of procedures for extrapolation to the complete basis set limit and explicitly correlated MP2 calculations; Cartesian coordinates and energies of all calculated structures; complete ref 68. This material is available free of charge via the Internet at http://pubs.acs.org.

JA807695P

---

(75) Claeyssens, F.; Harvey, J. N.; Manby, F. R.; Mata, R. A.; Mulholland, A. J.; Ranaghan, K. E.; Schütz, M.; Thiel, S.; Thiel, W.; Werner, H.-J. *Angew. Chem., Int. Ed.* **2006**, *45*, 6856–6859.